THE UNIVERSITY OF OKLAHOMA

GRADUATE COLLEGE

TIME DEPENDENCE OF PASSIVATING CURRENT FOR ANODIC PROTECTION

A THESIS

SUBMITTED TO THE GRADUATE FACULTY

in partial fulfillment of the requirements for the

degree of

MASTER OF SCIENCE

BY

LINO JUAN CARRILLO URDANETA

Norman, Oklahoma

1981

TIME DEPENDENCE OF PASSIVATING CURRENT DENSITY FOR ANODIC PROTECTION

A THESIS

APPROVED FOR THE SCHOOL OF CHEMICAL ENGINEERING AND MATERIALS SCIENCE

By

ACKNOWLEDGEMENT

I would like to express my most sincere appreciation to all those that helped me culminate successfully my graduate studies. I would especially thank:

Dr. Carl E. Locke, for all his help throughout my research, and especially for his support and direction during the preparation of this manuscript;

Dr. Raymond D. Daniels, for his participation on the Examination Committee;

Dr. John M. Radovich, for his participation on the Examination Committee;

K. Hudson, for his patient assistance and skillfull advice in the machine shop;

Jackie Elliott, for her superior typing of this manuscript;

Rosy de Doe, for her excellent photographs;

My wife and parents, for their continued encouragement throughout my graduate studies.

ABSTRACT

This study was conducted to investigate the time dependence of the critical current density for anodic protection. The systems studied were AISI 1018 carbon steel in 67 percent and 93 percent H_2SO_4, and Type 316 s/s in 67 percent H_2SO_4.

Potentiodynamic polarization was used to obtain data for both systems. Plots of the logarithm of the critical current density (i_{crit}) versus the logarithm of the time to passivate were made. From these plots the current-time relations for the systems were obtained. The equations describing the data for carbon steel in 67 percent and 93 percent H_2SO_4 were substantially different; this indicates that the passive film on carbon steel in 67 percent H_2SO_4 is electrically different from the film formed in the 93 percent acid. On the other hand, the equations for the carbon and stainless steel in 67 percent H_2SO_4 were very similar; this implies that both films have similar electrical properties in this acid.

For the stainless and carbon steels in 67 percent H_2SO_4, the critical current density changed slightly compared to more pronounced changes in the time to passivate. For the carbon steel in the 93 percent acid, more proportional changes were observed for the current density with respect to time.

Galvanostatic passivation was also used in this study in order to predict the effects of anode surface area on the critical current density and its time dependence. The results indicate that there is no relation whatsoever between the anode surface area and the critical current density; instead, it is the polarization technique used that affects the results obtained. The equation describing the galvanostatic (constant current) data resembled the equations obtained with the potentiodynamic technique. However, lower current densities were observed with the former.

TABLE OF CONTENTS

LIST OF TABLES

LIST OF FIGURES

CHAPTER I

INTRODUCTION

Anodic protection is an electrochemical technique for corrosion control which has been successfully applied in the chemical process industry for controlling the corrosion rate of storage tanks, process vessels, and process equipment.

Anodic protection can only be applied to metals and alloys that depict an active-passive behavior when a positive current is impressed upon them in the presence of a corrosive solution. Well-established examples are carbon and stainless steels in sulfuric acid media. The active-passive behavior of a metal or alloy is derived from the phenomenon of passivity. Passivity has been defined by Fontana and Greene(1) as the loss of chemical reactivity under conditions in which severe attack can be expected. This condition of chemical inertness of some metals in some corrosive solutions can be present naturally, or it can be induced by anodic polarization.

Anodic polarization of a metal that shows an active-passive behavior can be used by the corrosion or materials engineer to obtain all the electrochemical parameters needed to design an anodic protection system. The most important parameters are the critical current density (i_{crit}), the current density to maintain passivity (i_p), the primary

passivating potential (Epp), and the passivity potential range (see Figure (1)). When a system is anodically polarized, it first actively dissolves (active region) until it reaches Epp; at this point, the onset of passivity occurs. The system, then, is said to be passive and remains so until the transpassive region is reached. The transpassive region is characterized by oxygen evolution typical of transpassive dissolution. The main purpose of an anodic protection system is to take a metal in a corrosive solution from its active state to the passive state and to keep it there.

Anodic polarization curves are governed by the composition of the metal and the type and characteristics (flow, temperature, concentration, etc.) of the corrosive environment (2). Other characteristics of the system like time to passivate and anode/cathode area ratio also affect the shape and position of the polarization curve (see Figure 1). Of all the "characteristics" that influence a polarization curve, time has been the one that has received the least consideration among researchers in the field.

The time parameter referred to above is the time to achieve passivity, which along with the passivating current can be used to optimize the performance of an anodic protection system. Other researchers in the field (2) have suggested an inverse relationship between the time to passivate and the passivating current. That is, the higher the value of the current, the shorter the time to reach passivity

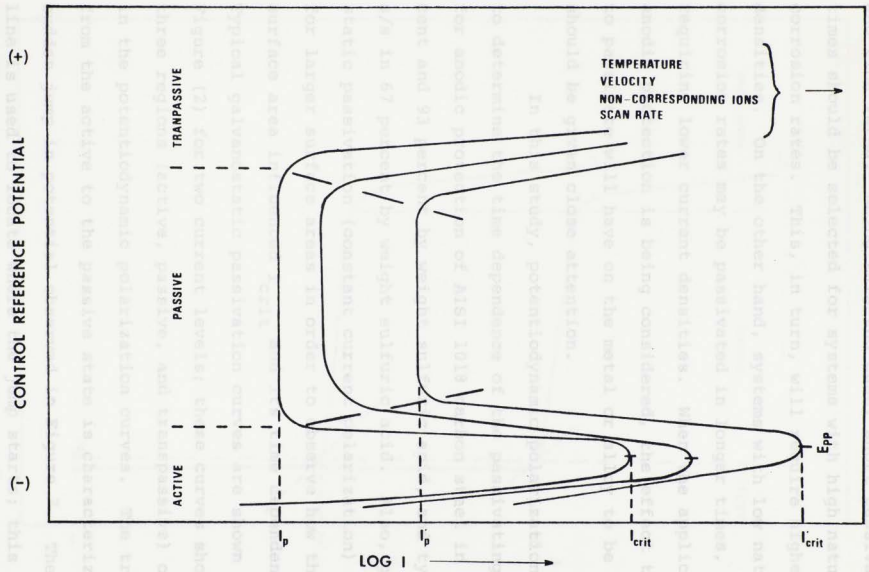

Figure 1 - Effects of Temperature, Velocity, Non-Corresponding Ions, and Scan Rate on Anodic Polarization of an Active-Passive Alloy.

and vice versa. Being this the case, short passivation times should be selected for systems with high natural corrosion rates. This, in turn, will require higher current densities. On the other hand, systems with low natural corrosion rates may be passivated in longer times, thus requiring lower current densities. When the application of anodic protection is being considered, the effect that time to passivate will have on the metal or alloy to be protected should be given close attention.

In this study, potentiodynamic polarization was used to determine the time dependence of the passivating current for anodic protection of AISI 1018 carbon steel in 67 percent and 93 percent by weight sulfuric acid, and type 316 s/s in 67 percent by weight sulfuric acid. Also, galvanostatic passivation (constant current polarization) was used for larger surface areas in order to observe how the anode surface area influenced i_{crit} and its time dependence, too. Typical galvanostatic passivation curves are shown in Figure (2) for two current levels; these curves show the three regions (active, passive, and transpassive) observed in the potentiodynamic polarization curves. The transition from the active to the passive state is characterized by the sudden jump in potential observed in Figure 2. The 45° line is used to locate where the jump starts; this point corresponds to Epp. The transpassive region, on the other hand, is very similar to that of the polarization curves.

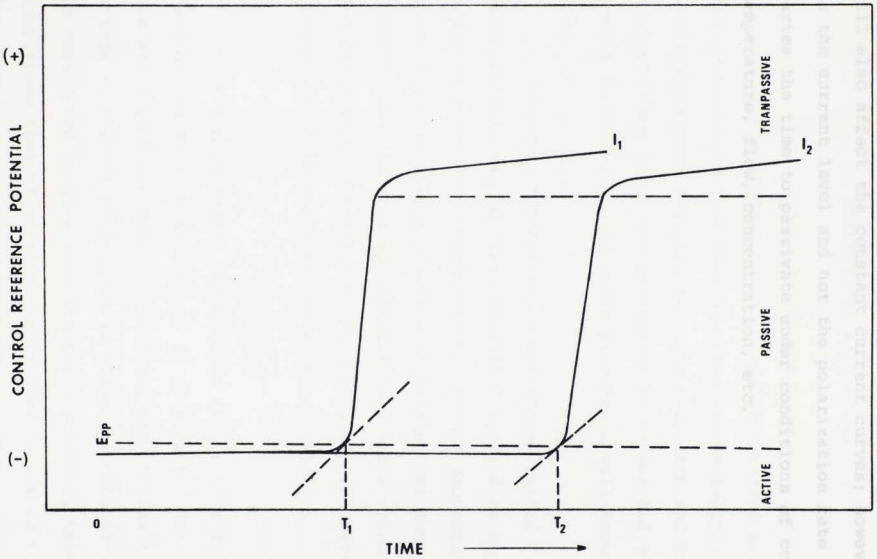

Figure 2 - Galvanostatic Passivation Curves of an Active-Passive Alloy for Two Different Current Levels.

Furthermore, the factors that affect the polarization curves will also affect the constant current curves; however, it is the current level and not the polarization rate that varies the time to passivate under conditions of constant temperature, flow, concentration, etc.

CHAPTER II

THEORETICAL BACKGROUND

Anodic Protection Theory

Anodic protection is an electrochemical technique for corrosion control that has been successfully used in the chemical process industry to solve corrosion and contamination problems (3). The protection of carbon and stainless steels in sulfuric acid media provides a well-known example (4).

Cathodic protection, a well-known method for corrosion control, can be "theoretically" applied to any metal or alloy in a corrosive environment. Anodic protection, on the other hand, is only applicable to metals that show an active-passive behavior when polarized toward noble potentials. The observed active-passive transition of some metals is brought about by a phenomenon called passivity.

Passivity

For many years, researchers in the corrosion field have argued about a definition of passivity. Two definitions are still in force today. The first one affirms that a metal active in the Emf Series, or an alloy composed of such metals, is considered passive when its electrochemical behavior approaches that of an appreciably less active or noble metal. The second one, on the other hand, considers a metal passive if it substantially resists corrosion in an environment

where thermodynamically there is a large free-energy decrease associated with its passage from the metallic state to appropriate corrosion products (5).

A thin film (10-100 Å) is said to be responsible for the active-passive behavior of some metal-solution systems. There exists some disagreement on the mechanism of the formation of this "passive" film. From all this disagreement, two theories stand out. That of Uhlig (5) who asserts that the film is formed by a chemisorbed layer of oxygen which displaces the water molecules from the metal surface. The oxygen layer may subsequently react with the base metal to form an oxide reaction product. Bockris and Reddy (6), on the other hand, contend that dissolution of the metal occurs first, then a salt or hydroxide with limited solubility is formed. This salt or hydroxide is called the prepassive or precursor film which, at first, is an electronic insulator. This precursor film undergoes some sort of change (oxidation) that allows it to become an electronic conductor; this change is indicative of the formation of the passive film.

Whatever the mechanism of the passive film formation is, one thing is certain, and that is that this passive film exists and is responsible for the applicability of anodic protection.

Polarization Behavior

Before any decisions are made as whether or not to use an anodic protection system, an anodic polarization curve for the solution-metal system must be obtained. This curve is characteristic of each system and will indicate if the metal under consideration shows the active-passive transition essential for anodic protection to work. Polarization curves can be obtained by potentiostatic or potentiodynamic polarization. These techniques are extensively explained elsewhere (7).

The systems AISI 1018 carbon steel in 67 percent and 93 percent by weight sulfuric acid, and Type 316 s/s in 67 percent by weight sulfuric acid were chosen for this study because they display the active-passive transition when anodically polarized (toward noble potentials). Polarization curves for the mentioned systems can be seen in Figures 3, 4, and 5, respectively.

Figure 3 shows the polarization curve for Type 316 s/s in 67 percent sulfuric acid at a scan rate of 0.278 mV/sec at 22.5± 0.5°C. The three characteristic regions are present, namely, the active, passive, and transpassive. However, a "secondary" passivity is present at about 600 mV. This second peak corresponds to the following reaction (5)

$$2Cr + 7H_2O \longrightarrow Cr_2O_7^{--} + 14H^+ + 12e^-$$

A smaller peak, at about 100 mV, can also be observed. This peak is known as the passive current maximum; its

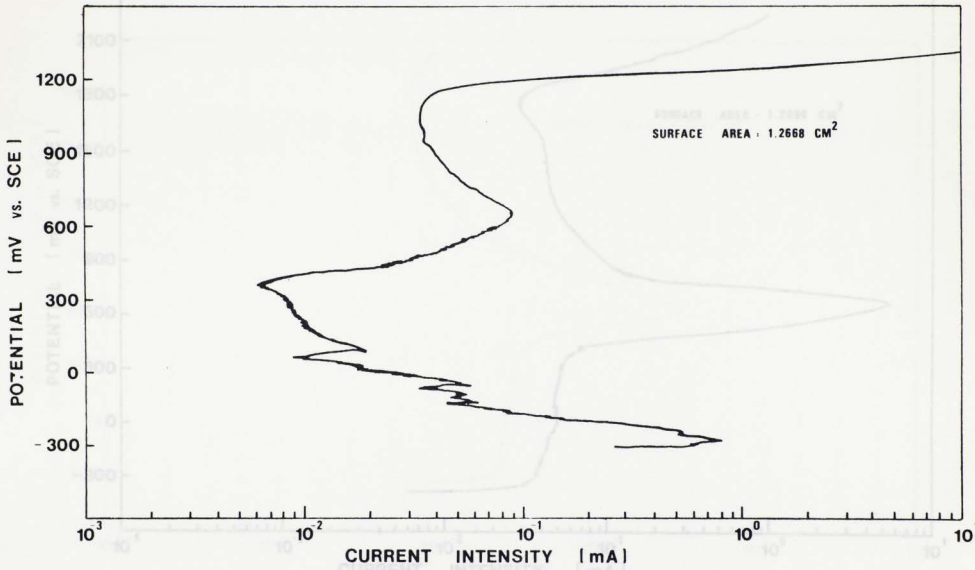

Figure 3 - Potentiodynamic Polarization of Type 316 s/s and 67% H_2SO_4 at 0.278 mV/sec and 22.5±0.5°C.

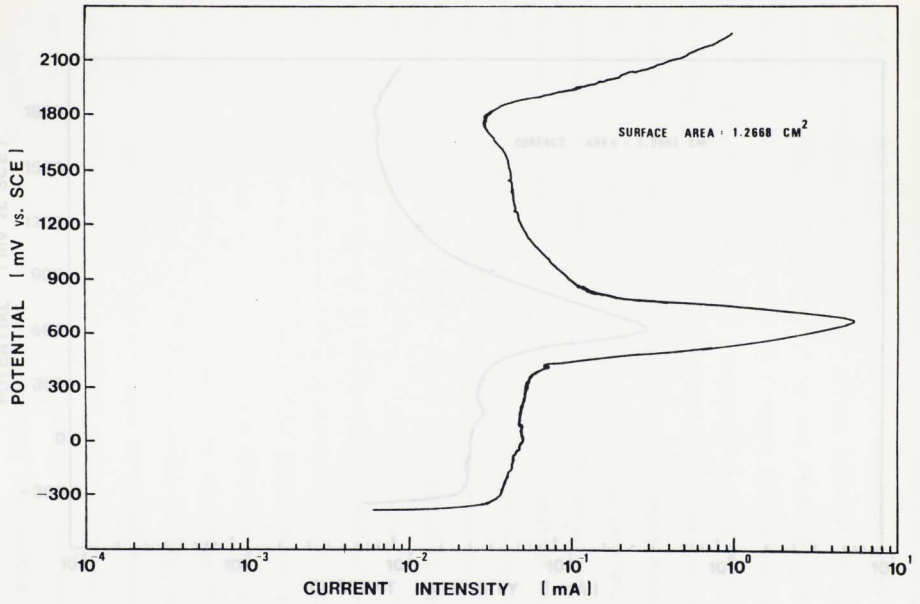

Figure 4 - Potentiodynamic Polarization of AISI 1018 Carbon Steel and 67% H_2SO_4 at 0.278 mV/sec and 22.5±0.5°C.

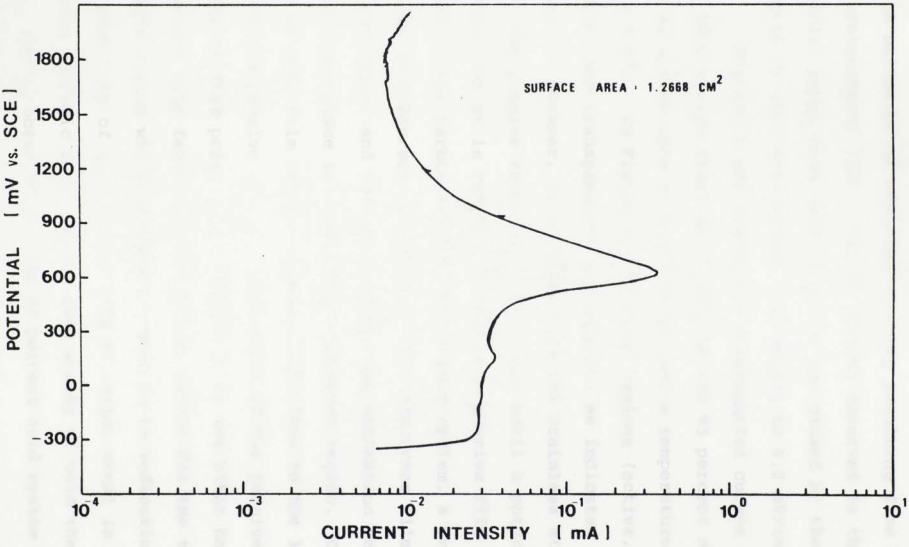

Figure 5 - Potentiodynamic Polarization of AISI 1018 Carbon Steel and 93% H_2SO_4 at 0.278 mV/sec and 22.5±0.5°C.

presence during potentiodynamic anodic polarization is due to oxidation of adsorbed hydrogen resulting from cathodic pretreatment (22). The serrations observed in the potential range from -100 to 300 mV are caused by the noise detected at slow scan speeds (0.1 mV/sec to 0.5 mV/sec).

Figures 4 and 5 show the polarization curves for AISI 1018 carbon steel in 67 percent and 93 percent sulfuric acid at a scan rate of 0.278 mV/sec and a temperature of 22.5$\pm$ 0.5°C. In Figure 4, the three regions (active, passive, and transpassive) are present, as indicated in Figure 1. However, in contrast with the stainless steel case, the passive region does not start until a potential of about 800 mV is reached. Before the passive film is formed in the carbon steel-sulfuric acid system, a prepassive or precursor film forms. This precursor film is a sulphate film, and the region where its nucleation and growth take place is called the sulphation region. Oxidation of this film begins at potentials close to the lower end of the passive region. Nucleation of the passive film begins at this point (21). Figure 5, on the other hand, shows the same features as Figure 4, except for the transpassive region which is absent. This is an indication of the stability of the passive film of carbon steel in 93 percent sulfuric acid. It is also worthy of note the lower i_{crit} and i_p observed for the 93 percent acid system as compared to the 67 percent acid case.

The differences among the behavior of each system are attributed mainly to the effects of acid concentration (8,9), and alloy constituents (10). Other factors (8,9,12, 13) that also govern the shape and position of the polarization curve are temperature, velocity, non-corresponding ion concentration, and the factor treated arbitrarily (11) by most researchers, the polarization rate. An increase in these variables tends to increase the current densities required to obtain and maintain passivity (2). Figure (1) shows this phenomenon.

Most of the research up to now has not dealt effectively with the influence of the polarization rate or time to passivate on the passivating current. Some work has been done on nickel (14,15), iron (11), and Type 304 s/s and titanium (10) in dilute sulfuric acid.

Chatfield, et al. (14) studied the effect of sweep rate on the active-passive transition of the Ni/H_2SO_4 system. In such study, Chatfield stressed that the increase of the passivating current density as the sweep rate was increased was due to the suppression of the anodic filming reactions so that dissolution continued at higher potentials than at slower sweep rates. The dissolution and filming reactions were assumed as follows:

(dissolution) $Ni \longrightarrow Ni^{2+}\ aq + 2e$

(filming) $Ni + 2H_2O \longrightarrow 2Ni(OH)_2 + 2H^+ + 2e$

According to Bockris, et al. (6), nickel hydroxide is the

precursor film for nickel. The hydroxide oxidizes and then becomes the passive film. So, any factor that retards the precipitation of nickel hydroxide will also retard the onset of passivation. The time at the reversible potential (open circuit potential) greatly influences the passivation process. At slow sweep rates (longer times), time at the reversible potential is sufficient for the rate-determining step for the formation of the passive film (nickel oxide) to occur, and it is possible that this rate-determining step involves the diffusion of H_2O dipoles and OH^- ions to the electrode-electrolyte interface. At higher sweep rates, the time available for nucleation of the oxide at the reversible potential is insufficient, and active dissolution continues until a higher potential is reached where the rate of oxide nucleation exceeds that of active dissolution. Nickel and carbon steel have similar polarization curves, thus similar behavior to that of nickel would be expected for the steel.

Reinoehl, et al. (11) gives a more quantitative analysis of the phenomenon controlling the increase of the passivating current with sweep rate. Reinoehl worked with single crystals and polycrystalline specimens of high purity and sulfurized iron in $1\underline{N}$ H_2SO_4. He emphasized the effect of polarization rate on the characteristic currents of the anodic polarization curve. He observed a logarithmic variation of the characteristic currents with polarization rate.

The relation is as follows:

$$i_x = \kappa(\dot{\eta})^{r}/_{\text{Temperature}} \qquad (1)$$

where κ and r are constants, i_x is any characteristic current density, and $\dot{\eta}$ is the polarization rate. The exponent r is called the polarization-rate-sensitivity. Its possible theoretical significance may be studied, according to Reinoehl, by means of the classical electrical circuit representation of a passive film, which is a resistance R and a capacitance C in parallel. The passive current is given by

$$i = \frac{V}{R} + C\frac{dv}{dt} \qquad (2)$$

where V is the potential difference across the passive film. Under transient conditions, the capacitive term of equation (2) predominates over the resistive term. Hence, at fast polarization rates, equation (2) may be approximated by

$$i = C\dot{\eta} \qquad (3)$$

This is true if the polarization rate reflects a change of the potential in the film.

At slower scan rates, the capacitive term may be neglected. The electrical behavior of the passive film is assumed to obey ohm's law, and the resistance to increase in proportion to the film thickness.

The film thickens in proportion to the current i but dissolves in proportion to i_o. Thus,

$$\frac{dR}{dt} = a(i-i_o) \qquad (4)$$

Equation (2) can then be written as

$$V_o + (\frac{\partial V}{\partial t})t = iR_o + i[a(i-i_o)t] \quad (5)$$

since $V_o = iR_o$, equation (5) can be simplified to

$$(\frac{\partial V}{\partial t})t = i[a(i-i_o)t] \quad (6)$$

and since $\dot{\eta} \approx \frac{\partial V}{\partial t}$, then

$$\dot{\eta} \approx i[a(i-i_o)] \quad (7)$$

If the passive film forms much more rapidly than it dissolves, then i_o can be neglected and equation (7) becomes

$$\dot{\eta} \approx i(ai) = ai^2 \quad \text{or}$$
$$i \cong A(\dot{\eta})^{\frac{1}{2}} \quad (8)$$

However, if i_o cannot be neglected, the exponent of $\dot{\eta}$ in equation (8) becomes correspondingly greater than one half.

Another method, discussed in a later chapter, called galvanostatic passivation, can also be used to obtain data to determine a relationship for the dependence of the passivating current on the passivating time instead of the scan rate. Under ideal conditions (very slow scan rates, 1 mV/min-12 mV/min), the passivating time is inversely proportional to the scan rate; at faster scan rates their relation varies some.

According to Reinoehl, et al. (11), the equations that describe galvanostatic passivation are as follow:

$$(i-i_{crit})t^{\frac{1}{2}} = \kappa \quad (9)$$

and

$$(i-i_{crit})t = Q \quad (10)$$

In equations (9) and (10), i is the imposed galvanostatic current, i_{crit} is the critical current for passivation (equilibrium value), and κ and Q are constants. Equation (9), like (8), corresponds to long times (slow scan rates), and equations (10) and (3) to short times (fast scans).

Polarization-rate-sensitivities greater than one are not conceivable under the present analysis. A more refined electrical model such as that proposed by Engell and Ilsehner (17) may be required to explain these data (as referred to by Reinoehl's article (11)).

In the literature, only Banks, et al. (12) presents a summary of one combination of field and laboratory data. Banks suggests a marked dependence of i_{crit} on the time to passivation (see Figure 6), and also on the anode surface area. According to Figure 6, a plot of the logarithmic of i_{crit} versus the passivation time should be linear. On the other hand, Sudbury, et al. (13) have also suggested the dependence of i_{crit} on the anode surface area. Sudbury found that i_{crit} decreased with increasing surface area up to about 200 inches squared, and then remained constant for larger areas (see Figure 7). The decrease in current density with the surface area may be caused by the change of polarization technique used for small (coupons) and larger (tanks) areas. Or, it may be that, since high power potentiostats are used for large surface areas, these may not be as accurate when operated at very low current outputs corresponding to the smaller surface areas.

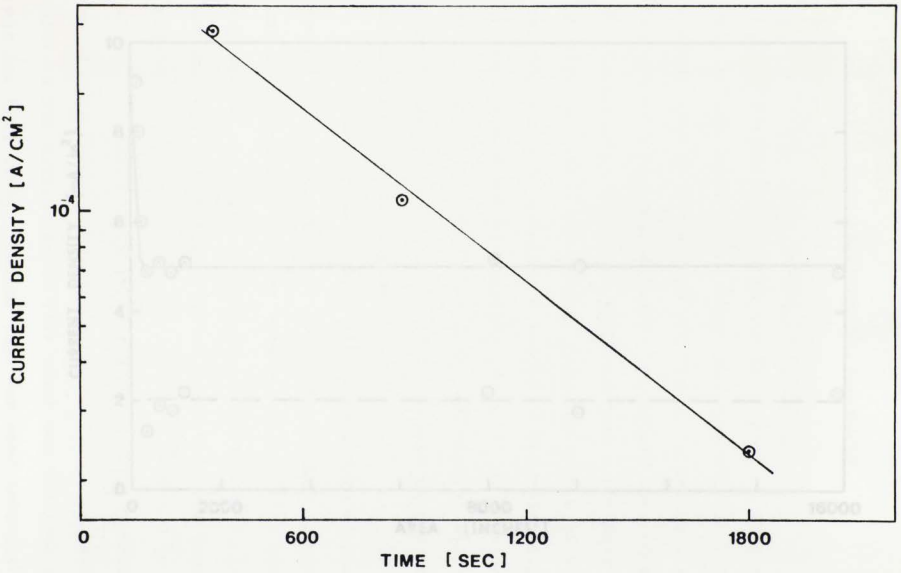

Figure 6 - Semi-log Plot of i_{crit} versus Time to Passivation of Bank's Field Data on Carbon Steel and 93% H_2SO_4.

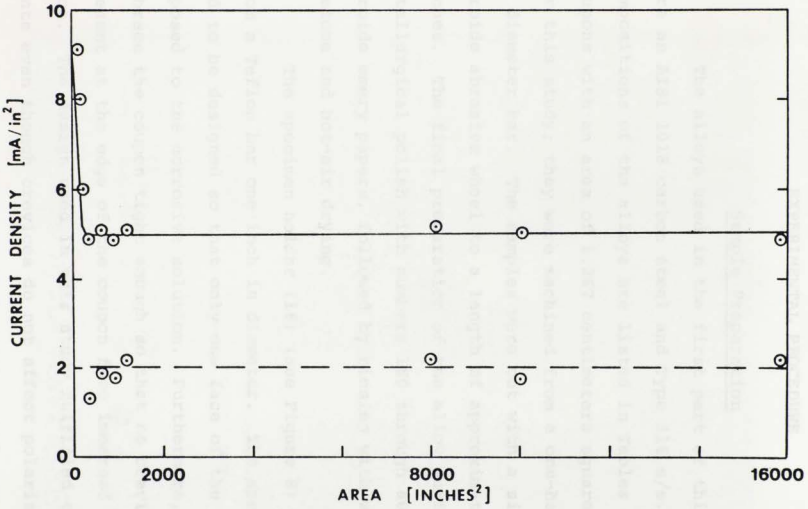

Figure 7 - Influence of Anode Surface Area on i_{crit}, Sudburry's Data.

CHAPTER III

EXPERIMENTAL PROCEDURE

Sample Preparation

The alloys used in the first part of this study were an AISI 1018 carbon steel and Type 316 s/s. Chemical compositions of the alloys are listed in Tables 1 and 2. Coupons with an area of 1.267 centimeters squared were used for this study; they were machined from a one-half inches in diameter bar. The samples were cut with a silicon carbide abrasive wheel to a length of approximately one-half inches. The final preparation of the alloy surface was a metallurgical polish with numbers 180 through 600 silicon carbide emery papers, followed by rinsing with water and acetone and hot-air drying.

The specimen holder (18) (see Figure 8) was made from a Teflon bar one inch in diameter. The specimen holder had to be designed so that only one face of the coupon was exposed to the corrosive solution. Furthermore, it had to embrace the coupon tight enough so that no crevices were present at the edge of the coupon face immersed in the solution. The design used in this study fulfilled these requirements even though crevices do not affect polarization behavior in the active region (19) which was the zone of interest for this study. Teflon tape was used around the coupons to obtain better protection at the edges. The samples were

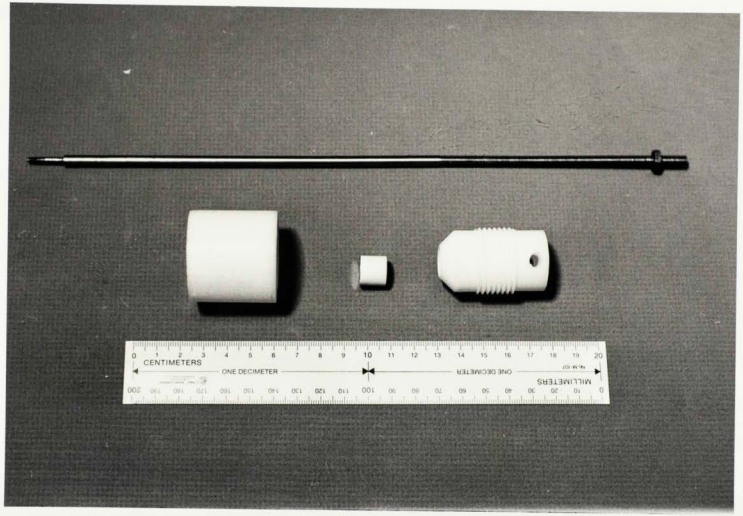

Figure 8 - Specimen Holder

TABLE I

Chemical Composition of 1018 Carbon Steel in Weight Percent

	Carbon	Manganese	Phosphorus	Sulfur
Maximum	0.13	0.30	0.04	0.05
Minimum	0.18	0.60	----	----

TABLE II

Chemical Composition of Type 316 s/s in Weight Percent

C	Mn	P	S	Si	Cr	Ni	Mo*	Cu	Co
0.018	1.93	0.029	0.017	0.61	17.37	11.15	2.09	0.24	0.17

*The coupons had a 4.0 percent Mo content.

inserted in the nut-like piece shown in Figure 8. Then they were screwed in the case which exerted enough pressure on the tip of the nut-like piece to prevent any solution from wetting any other area than the face area. A ten inches long steel rod was threaded to the other face of the sample in order to hold the sample still in the solution and serve as electrical extension for the sample, too.

The solutions used were 67 percent and 93 percent by weight sulfuric acid. They were made from 96 percent by weight, analytical grade sulfuric acid, and distilled water from the University power plant.

For this second set, cold drawn seamless MTX-1015 (C-1018) carbon mechanical steel tube, 8 inches in diameter and one foot long, and stress relieved to ASTM-A-519 was used to make a bucket. The material was purchased at Kilsby Tube Supply Company, Tulsa, Oklahoma. The bottom of the bucket was cut from flat stock equivalent to 1018 carbon steel, one-half inch thick, purchased at Ducommun Metals Company in Oklahoma City. The plate was cut to fit exactly to the pipe outside diameter in order to facilitate the welding of the parts. Helium-arc welding, without any filler metal, was used to join the two parts. A 316 s/s bucket was also made. A one foot long, 6 inches in diameter, A-312 full finish T-316 s/s pipe single RML was used. The material was purchased at the same company the carbon steel pipe was. The bottom of the bucket was available at the

machine shop; it was 3/32 inches thick.

It was impossible to mechanically clean the buckets; so, an electrochemical technique called cathodic pretreatment was used instead. This cathodic pretreatment is a combination of chemical cleaning provided by a mineral acid (or a mixture of acids), and an electrical cleaning (descaling) provided by impressing a cathodic (-) current on the alloy-acid system for a certain period of time. For the 67 percent sulfuric acid experiments, 67 percent sulfuric acid was used as the chemical cleaner; while for the 93 percent acid experiments, 93 percent acid was used. For the electrical cleaning, the criterion was to apply enough current to the alloy-acid system so that its potential was shifted to -500 mV versus SCE, where active dissolution of the alloy took place. The system was then held at this potential for five minutes; this time was enough to dissolve any oxide or passive film formed on a previous experiment and to activate the surface of the bucket exposed to the acid. Clean acid solutions were used after cathodic pretreatment to obtain data from the buckets.

The acid concentrations used in this second set of experiments were the same as for the first set. However, two volumes of acid were used, 1825 and 3650 milliliters, corresponding to surface areas of 661.15 and 1140.42 centimeters squared, respectively.

Polarization Tests

Two types of polarization techniques were used, namely potentiodynamic polarization and galvanostatic passivation.

Potentiodynamic polarization is a continuous technique in which the potential is changed at a constant rate. This technique is favored by many researchers over the potentiostatic technique because it is less time consuming than the latter. The instrumentation used to conduct the tests was an EG&G Princeton Applied Research Model 175 Universal Programmer, an EG&G Princeton Applied Research Model 173 Potentiostat/Galvanostat with a Model 376 Logarithmic Current Converter plug-in module, and a Hewlett-Packard Model 7044A, x-y chart recorder (see Figure 9). Due to the small power output of this system, potentiodynamic polarization was only performed on the small samples.

The polarization cell used was one proposed by Greene (20), consisting of a six-necked 1,000 milliliter round bottom Pyrex flask (see Figure 10). Three holes were occupied by the sample (working electrode), a saturated calomel electrode (for potential reference), and a platinum auxiliary electrode. The other three holes were closed with glass stoppers. This simulates the enclosed atmosphere of sulfuric acid storage tanks. Before any polarization was performed, one hour was allowed for sample equilibration at room temperature (22.5 $\pm$ 0.5°C).

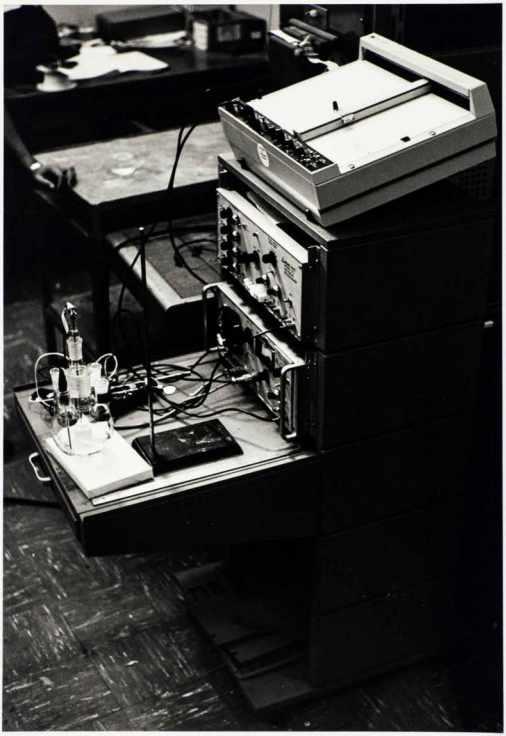

Figure 9 - Potentiodynamic Polarization Unit with Recorder

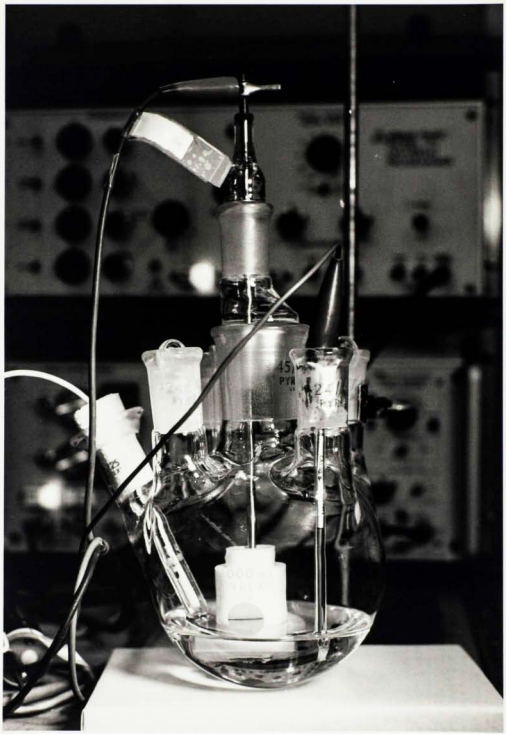

Figure 10 - Polarization Cell

Galvanostatic passivation, on the other hand, is the technique still in use in most field applications of anodic protection. Potentiodynamic polarization is more powerful than galvanostatic passivation; however, the results obtained using the former are not always easy to interpret (21). In galvanostatic passivation, a constant current (d.c.) is applied to the system under study, the potential of the working electrode is then recorded as a function of time.

The instrumentation used for the small samples was the same used for the potentiodynamic polarization, except that the programmer was turned off and the X-axis of the recorder was used as a time axis instead of a logarithmic scale for the current density. The instrumentation used for the buckets was a power supply, provided by the electrical engineering shop, rated at 5 volts and 30 amps. A variable resistance box (variac) was used to adjust the output of the power supply (see Figure 11). This equipment was not the most suitable for the kind of data that needed to be taken. This is so because as the passive film formed, the resistance of the system increased, and then more driving force (voltage) was needed from the power supply. The increase in the output had to be made manually and could not be made automatically; this, of course, introduced noticeable inaccuracy. It would have been less time consuming, more accurate, and more reproducible if a high power

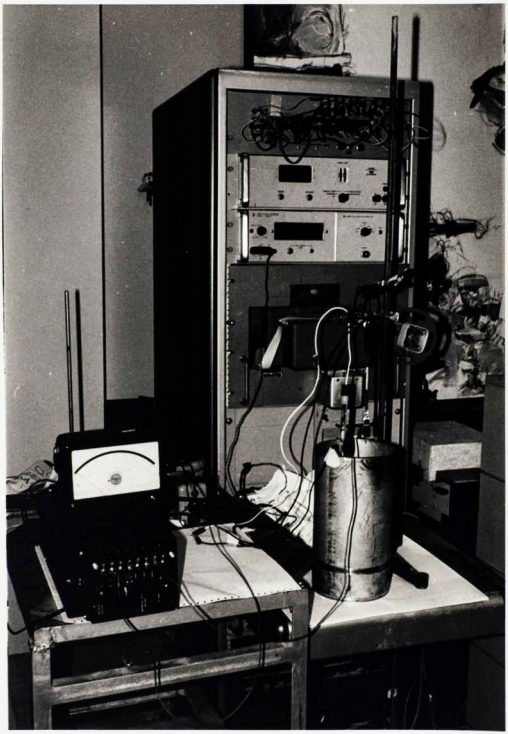

Figure 11 - Galvanostatic Passivation Unit with Bucket

potentiostat were available.

Galvanostatic passivation was used with both the coupons and the buckets in order to make sure that the area and not the polarization technique was the cause for the difference between the results for each case.

CHAPTER IV

RESULTS AND DISCUSSION OF RESULTS

The results obtained for the coupons and the buckets are presented in this section. Discussion of the results is centered around the data obtained with the coupons using potentiodynamic polarization and galvanostatic passivation, and the data obtained with the buckets using galvanostatic passivation.

Potentiodynamic Polarization

Potentiodynamic polarization curves were obtained for both systems, 1018 carbon steel and Type 316 s/s. For the carbon steel, two acid concentrations, 67 percent and 93 percent by weight, were used, while for the stainless steel only the 67 percent concentrated acid was used (in 93 percent acid the stainless steel self-passivates). See Figures 12, 13, and 14 for the anodic scans.

Figure 12 depicts the anodic polarization curves for Type 316 s/s in 67 percent sulfuric acid. As the scan rate is increased (short passivation times), i_{crit} increases, too. Some researchers have found that the formation of the passive film requires a constant amount of charge (Q); since charge is related to the applied current and to the time the current is applied ($Q=\int_o^t idt$), then a decrease/increase of the scan rate (the inverse of the time to passivation) has to be offset by a decrease/

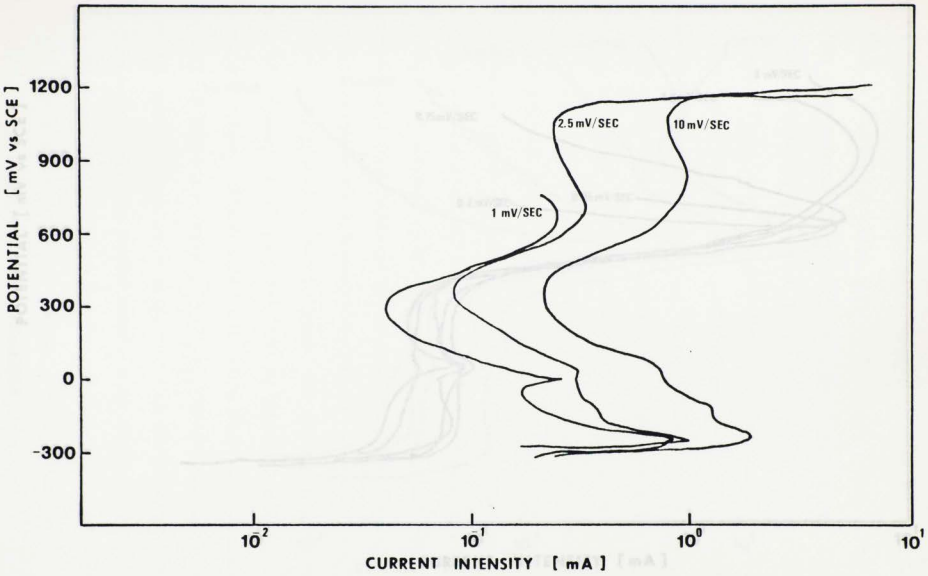

Figure 12 - Potentiodynamic Polarization Curves for Type 316 s/s and 67% H_2SO_4.

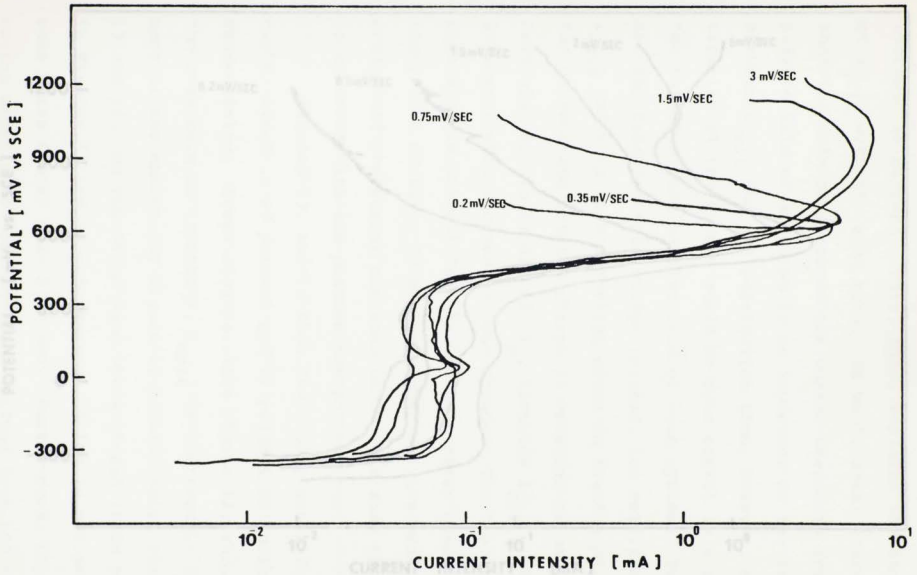

Figure 13 - Potentiodynamic Polarization Curves for AISI 1018 Carbon Steel and 67% H_2SO_4.

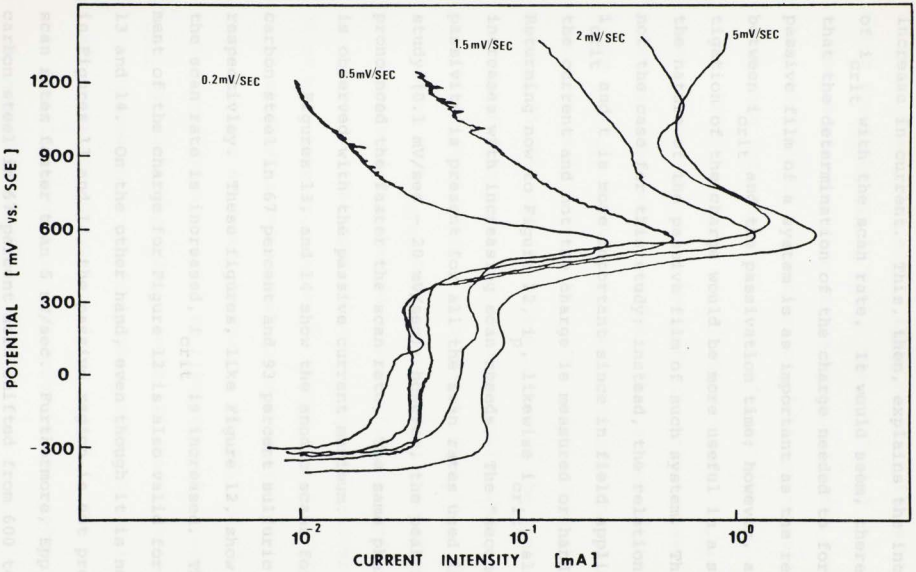

Figure 14 - Potentiodynamic Polarization Curves for AISI 1018 Carbon Steel and 93% H_2SO_4.

increase in current. This, then, explains the increase of i_{crit} with the scan rate. It would seem, therefore, that the determination of the charge needed to form the passive film of a system is as important as the relation between i_{crit} and the passivation time; however, an investigation of the charge would be more useful in a study of the nature of the passive film of such system. This is not the case for this study; instead, the relation between i_{crit} and t is more important since in field application the current and not the charge is measured or handled. Returning now to Figure 12, i_p, likewise i_{crit}, also increases with increasing scan speeds. The "secondary" passivity is present for all the scan rates used in this study (0.1 mV/sec - 20 mV/sec); however, the peak is less pronounced the faster the scan rate. The same phenomenon is observed with the passive current maximum.

Figures 13, and 14 show the anodic scans for 1018 carbon steel in 67 percent and 93 percent sulfuric acid, respectivley. These figures, like Figure 12, show that as the scan rate is increased, i_{crit} is increased. The argument of the charge for Figure 12 is also valid for Figures 13 and 14. On the other hand, even though it is not shown in Figures 13 and 14, the passive region is not present at scan rates faster than 5 mV/sec. Furthermore, Epp for the carbon steel in 67 percent acid shifted from 600 to 1000 mV versus SCE as the sweep rate was increased from 0.2 to 3.0

mV/sec. Chatfield, et al. (14), observed the same phenomenon for Nickel in 1N H_2SO_4. He attributed this to the influence of sweep rate on the kinetic factors involved in the precipitation and nucleation of the pre-passive film, which then influences the onset of passivity.

From the anodic polarization curves, i_{crit} and the time it took the system to reach the primary passivating potential (Epp) were recorded. Then a plot of the logarithm of i_{crit} versus the time to passivation was made (see Figures 15 through 17). The relationship shown in Figures 15, 16, and 17 was not linear on the semi-log plot as indicated in Figure 6. Similar results were obtained by Chatfield, et al. (14) with Nickel in 1N H_2SO_4. Chatfield also found that i_{crit} remained practically constant at sweep rates slower than 50 mV/min. In this study, i_{crit} approached a "limiting" value at scan rates slower than 30 mV/min; however, scan rates slower than 6 mV/min need to be studied in order to obtain a more accurate value of this limiting current. In Figures 15, 16, and 17, tentative curves were drawn in order to illustrate the approach of i_{crit} to a limiting value. Locke (23) has also observed this phenomenon in the field when trying to passivate (galvanostatic passivation) large vessels. The meaning of this limiting current is that below it the system under study cannot be passivated.

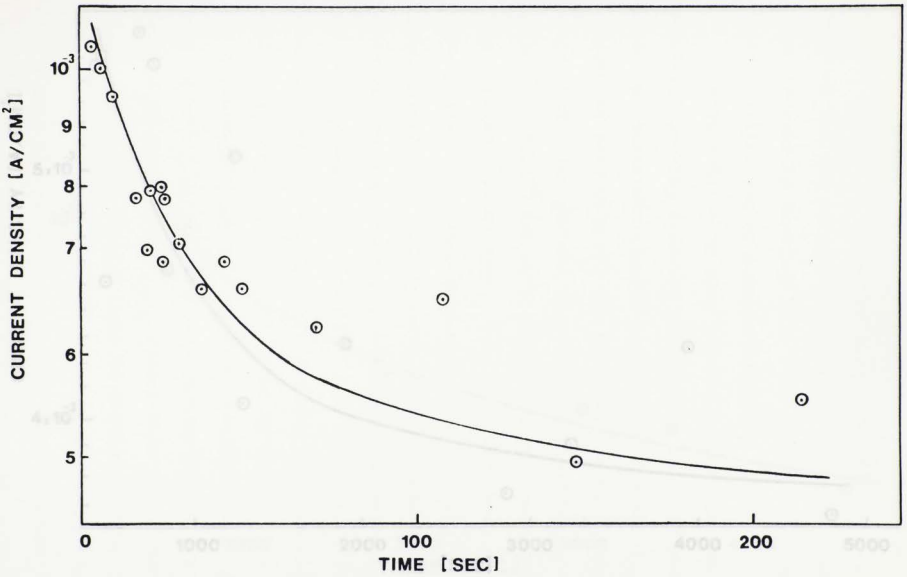

Figure 15 - Semi-log Plot of i_{crit} versus Time to Passivation for the Potentiodynamic Polarization Data for Type 316 s/s Coupons and 67% H_2SO_4.

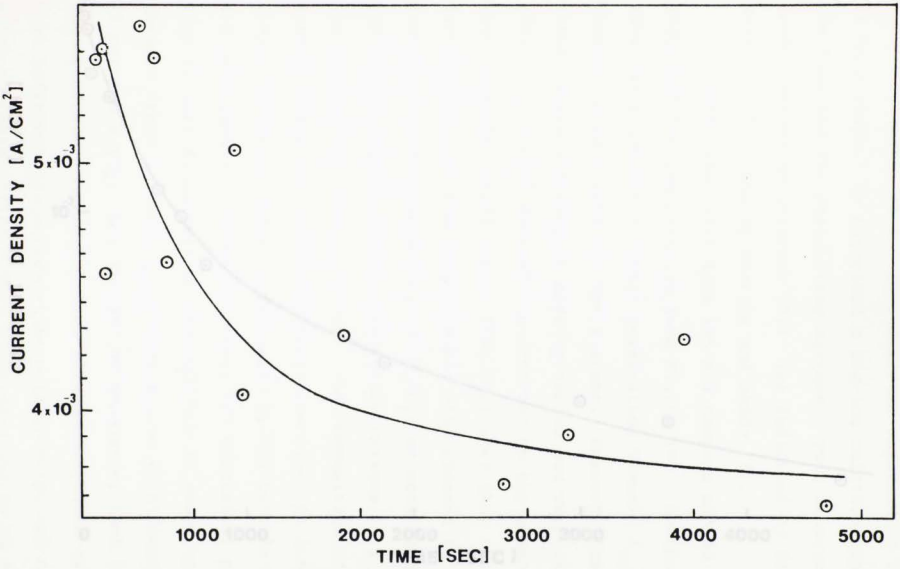

Figure 16 - Semi-log Plot of i_{crit} versus Time to Passivation for the Potentiodynamic Polarization Data for AISI 1018 Carbon Steel Coupons and 67% H_2SO_4.

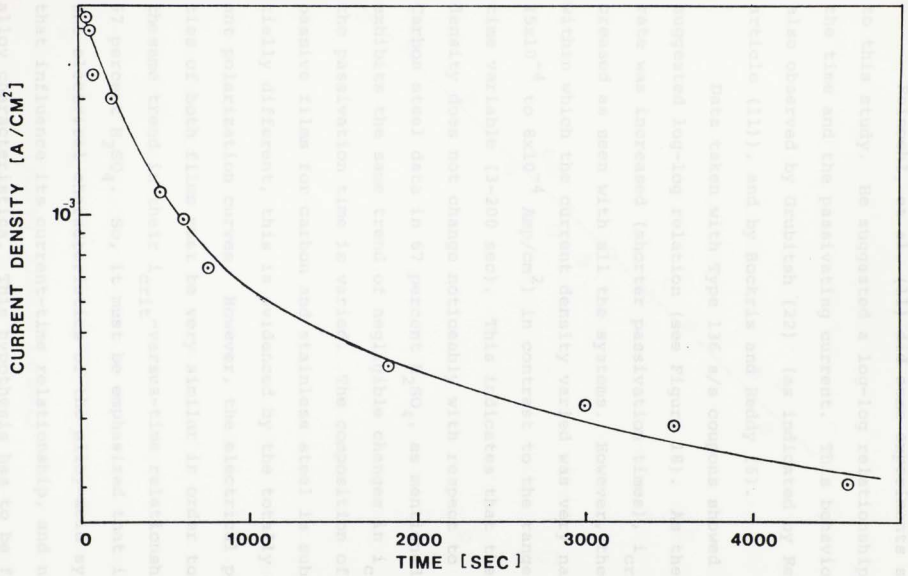

Figure 17 - Semi-log Plot of i_{crit} versus Time to Passivation for the Potentiodynamic Polarization Data for AISI 1018 Carbon Steel Coupons and 93% H_2SO_4.

Reinoehl, et al. (11) did some experiments similar to this study. He suggested a log-log relationship between the time and the passivating current. This behavior was also observed by Grubitsh (22) (as indicated by Reinoehl's article (11)), and by Bockris and Reddy (6).

Data taken with Type 136 s/s coupons showed the suggested log-log relation (see Figure 18). As the sweep rate was increased (shorter passivation times), i_{crit} increased as seen with all the systems. However, the range within which the current density varied was very narrow ($5x10^{-4}$ to $8x10^{-4}$ Amp/cm^2) in contrast to the range of the time variable (3-200 sec). This indicates that the current density does not change noticeably with respect to time. Carbon steel data in 67 percent H_2SO_4, as mentioned later, exhibits the same trend of negligible changes in i_{crit} as the passivation time is varied. The composition of the passive films for carbon and stainless steel is substantially different, this is evidenced by the totally different polarization curves. However, the electrical properties of both films must be very similar in order to explain the same trend in their i_{crit}-versus-time relationships in 67 percent H_2SO_4. So, it must be emphasized that it is the electrical characteristics of the alloy-acid system that influence its current-time relationship, and not the alloy characteristics. This hypothesis has to be further documented with experiments with other alloys like Nickel,

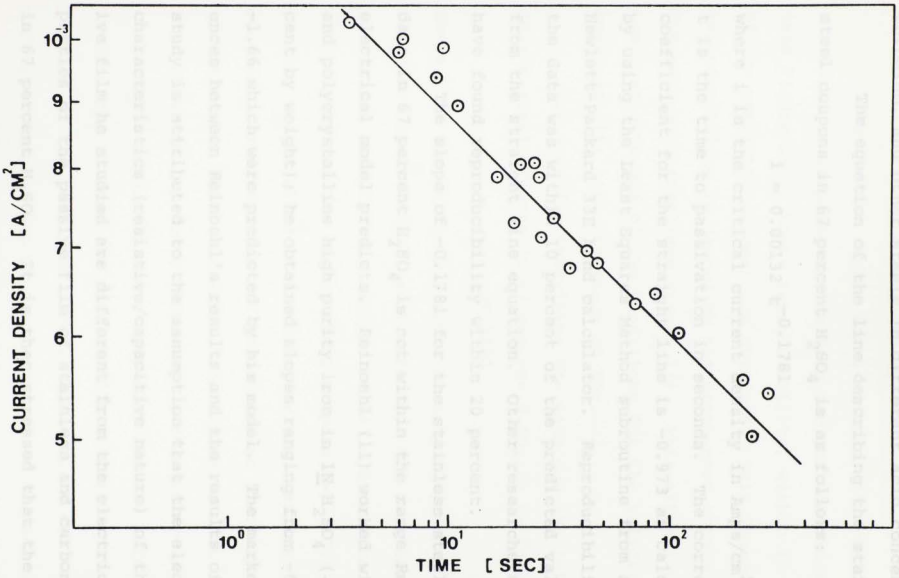

Figure 18 - Log-log Plot of i_{crit} versus Time to Passivation for the Potentiodynamic Polarization Data for Type 316 s/s Coupons and 67% H_2SO_4 (Same Data as in Figure 15).

Chromium, and other steels in different acid concentrations.

The equation of the line describing the stainless steel coupons in 67 percent H_2SO_4 is as follows:

$$i = 0.00132\ t^{-0.1781} \qquad (11)$$

where i is the critical current density in Amps/cm^2, and t is the time to passivation in seconds. The correlation coefficient for the straight line is -0.973 as calculated by using the Least Squares Method subroutine from a Hewlett-Packard 33E hand calculator. Reproducibility of the data was within 10 percent of the predicted values from the straight line equation. Other researchers (15) have found reproducibility within 20 percent.

The slope of -0.1781 for the stainless steel coupons data in 67 percent H_2SO_4 is not within the range Reinoehl's electrical model predicts. Reinoehl (11) worked with single and polycrystalline high purity iron in 1$\underline{N}$ H_2SO_4 (~4.7 percent by weight); he obtained slopes ranging from -0.5 to -1.66 which were predicted by his model. The marked differences between Reinoehl's results and the results of this study is attributed to the assumption that the electrical characteristics (resistive/capacitive nature) of the passive film he studied are different from the electrical properties of the passive film of stainless and carbon steel in 67 percent H_2SO_4. It is then stressed that the electrical properties of the alloy-acid system, and not the chemical composition of the passive film, greatly influence the

current-time relation for such system.

Data for the carbon steel coupons was considerably scattered as compared to the data for the stainless steel (see Figure 19). Lower reproducibility, within 15 percent of the predicted values, was obtained. This decrease in reproducibility is caused by the pronounced change of Epp with scan rate (see Figure 13). This situation is in contrast with one of the conditions for the validity of equation (1): the constancy of Epp.

The equation describing the data for the 1018 carbon steel coupons in 67 percent H_2SO_4 is as follows:

$$i = 0.0151\ t^{-0.1680} \qquad (12)$$

where i is the critical current density in Amps/cm^2, and t is the passivation time in seconds. The correlation factor for the straight line is -0.843. Since the slope of the line for the carbon steel coupons (-0.1680) is similar to the slope of the line for the stainless steel coupons, the discussion for the stainless steel applies to the carbon steel. However, the higher current densities observed for the carbon steel steel system ($3.6x10^{-3}$ to $5.4x10^{-3}$ Amps/cm^2) are as expected because more charge is required to form the passive film on carbon steel than it does on the stainless steel. This can be due to the different composition of the passive film of each system; this is evidenced by the different electrode potentials at which each film forms, which is probably characteristic

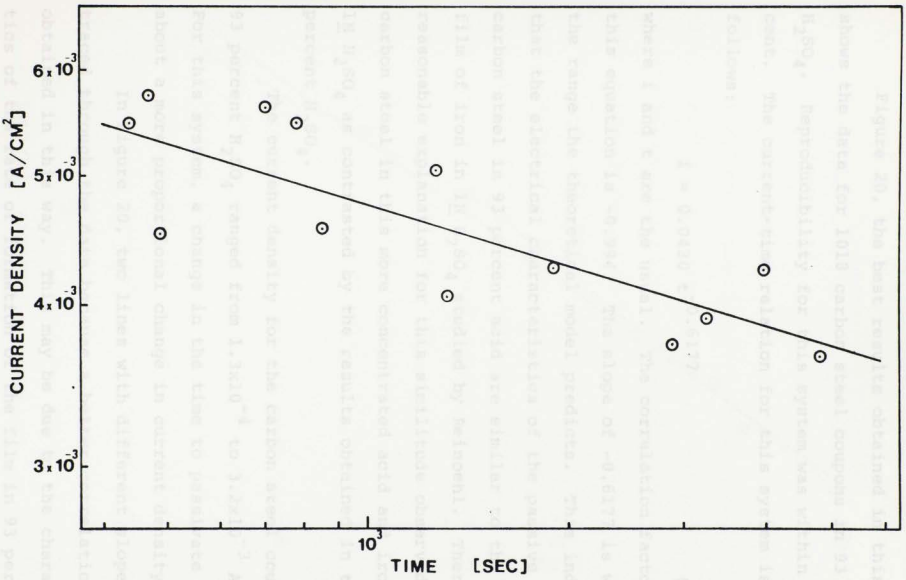

Figure 19 - Log-log Plot of i_{crit} versus Time to Passivation for the Potentiodynamic Polarization Data for AISI 1018 Carbon Steel Coupons and 67% H_2SO_4 (Same Data as in (Figure 16).

of the constituents of both alloys.

Figure 20, the best results obtained in this study, shows the data for 1018 carbon steel coupons in 93 percent H_2SO_4. Reproducibility for this system was within 5 percent. The current-time relation for this system is as follows:

$$i = 0.0430\ t^{-0.6177} \qquad (13)$$

where i and t are the usual. The correlation factor for this equation is -0.994. The slope of -0.6177 is within the range the theoretical model predicts. This indicates that the electrical characteristics of the passive film on carbon steel in 93 percent acid are similar to the passive film of iron in 1N H_2SO_4 studied by Reinoehl. There is no reasonable explanation for this similitude observed for carbon steel in this more concentrated acid and iron in 1N H_2SO_4 as contrasted by the results obtained in the 67 percent H_2SO_4.

The current density for the carbon steel coupons in 93 percent H_2SO_4 ranged from 1.3×10^{-4} to 3.2×10^{-3} Amps/cm^2. For this system, a change in the time to passivate brought about a more proportional change in current density.

In Figure 20, two lines with different slopes were traced through the data because a better correlation was obtained in this way. This may be due to the characteristics of the rate of formation of the film in 93 percent acid; a more detailed discussion on the topic is given in

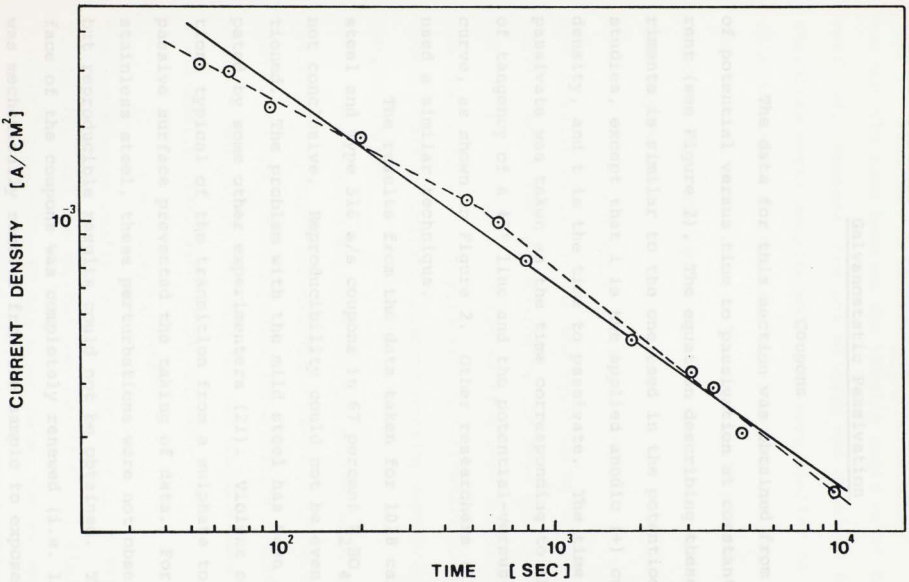

Figure 20 - Log-log Plot of i_{crit} versus Time to Passivation for the Potentiodynamic Polarization Data for AISI 1018 Carbon Steel Coupons and 93% H_2SO_4 (Same Data as in Figure 17).

the next section.

Galvanostatic Passivation

Coupons

The data for this section was obtained from plots of potential versus time to passivation at constant current (see Figure 2). The equation describing these experiments is similar to the one used in the potentiodynamic studies, except that i is the applied anodic (+) current density, and t is the time to passivate. The time to passivate was taken as the time corresponding to the point of tangency of a 45° line and the potential-versus-time curve, as shown in Figure 2. Other researchers (6) have used a similar technique.

The results from the data taken for 1018 carbon steel and Type 316 s/s coupons in 67 percent H_2SO_4 were not conclusive. Reproducibility could not be even mentioned. The problem with the mild steel has been anticipated by some other experimenters (21). Violent oscillations typical of the transition from a sulphate to a passive surface prevented the taking of data. For the stainless steel, these perturbations were not observed, but reproducible results could not be obtained. The surface of the coupons was completely renewed (i.e. 1 mm was mechanically removed from the sample to expose fresh metal) to rule out that depletion of one of the alloy

constituents was the cause of unreproducible results; it was not the case because the results could never be reproduced. However, one set of data was obtained for the stainless steel coupons which was very similar to the data obtained when the stainless steel bucket was used. Unfortunately, as said before, this data could not be reproduced at all. The equation for this data is as follows (see Figure 21):

$$i = 0.00116\ t^{-0.0763} \qquad (14)$$

The correlation factor for the equation is -0.987. Higher current densities as compared to the ones obtained in the potentiodynamic polarization section were obtained when the stainless steel coupons were galvanostatically passivated. This increase in current density cannot be reasonably explained.

The results obtained for the carbon steel in 93 percent H_2SO_4 under galvanostatic passivation were very similar to the potentiodynamic polarization results. The equation describing the data for the coupons when galvanostatically passivated is as follows:

$$i = 0.01437\ t^{-0.6495} \qquad (15)$$

The correlation coefficient for the line is -0.991 (see Figure 22), and the current was ranged from 1.18×10^{-4} to 7.89×10^{-4} Amps/cm^2. On the other hand, the curves for the galvanostatic passivation and potentiodynamic polarization data for the carbon steel coupons in 93 percent

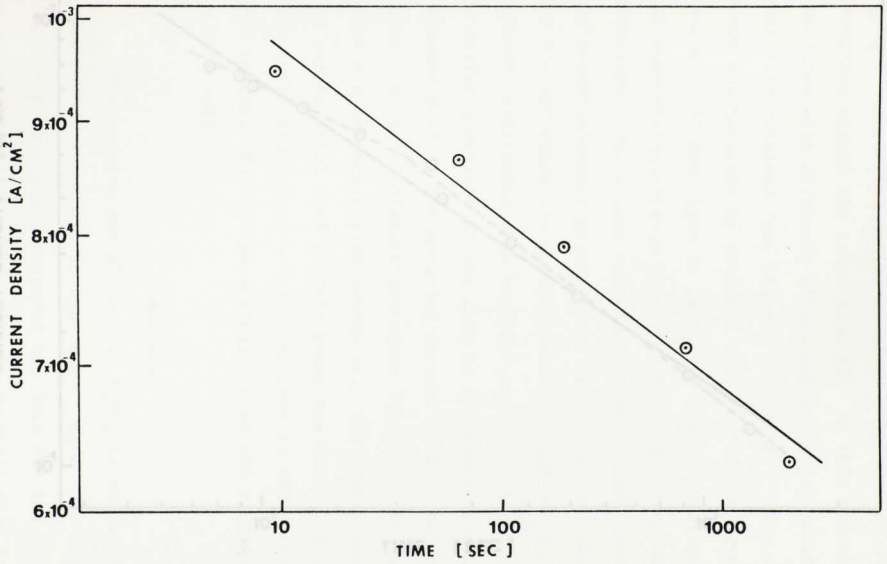

Figure 21 - Log-log Plot of i_{crit} versus Time to Passivation for the Galvanostatic Passivation Data for Type 316 s/s Coupons and 67% H_2SO_4.

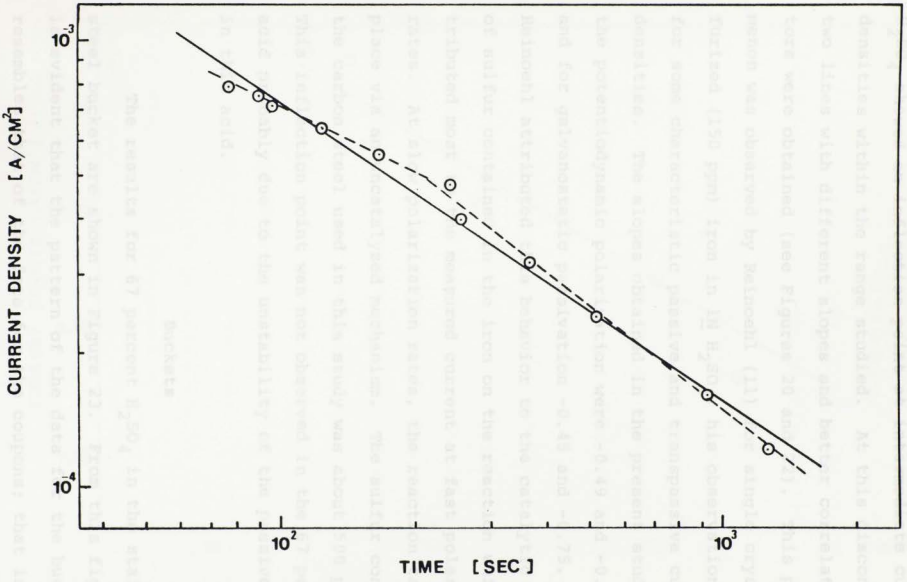

Figure 22 - Log-log Plot of i_{crit} versus Time to Passivation for the Galvanostatic Passivation Data for AISI 1018 Carbon Steel Coupons and 93% H_2SO_4.

H_2SO_4 showed an inflection point at intermediate current densities within the range studied. At this discontinuity, two lines with different slopes and better correlation factors were obtained (see Figures 20 and 22). This phenomenon was observed by Reinoehl (11) for single crystal sulfurized (150 ppm) iron in 1N H_2SO_4; his observations were for some characteristic passive and transpassive current densities. The slopes obtained in the present study for the potentiodynamic polarization were -0.49 and -0.67, and for galvanostatic passivation -0.45 and -0.75. Reinoehl attributed this behavior to the catalytic action of sulfur contained in the iron on the reaction which contributed most to the measured current at fast polarization rates. At slow polarization rates, the reaction takes place via an uncatalyzed mechanism. The sulfur content of the carbon steel used in this study was about 500 ppm. This inflection point was not observed in the 67 percent acid probably due to the unstability of the passive film in this acid.

Buckets

The results for 67 percent H_2SO_4 in the stainless steel bucket are shown in Figure 23. From this figure, it is evident that the pattern of the data for the bucket resembles that of the data for the coupons; that is, as the current was slightly varied, the time to passivate changed

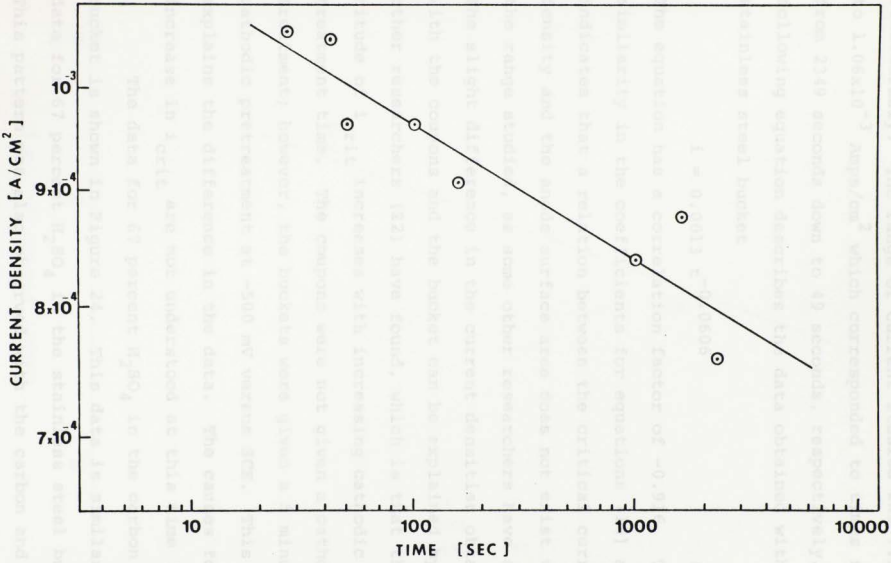

Figure 23 - Log-log Plot of i_{crit} versus Time to Passivation for the Galvanostatic Passivation Data for Type 316 s/s Bucket and 67% H_2SO_4.

considerably. The range of current studied was 7.56×10^{-4} to 1.06×10^{-3} Amps/cm^2 which corresponded to times ranging from 2349 seconds down to 49 seconds, respectively. The following equation describes the data obtained with the stainless steel bucket

$$i = 0.0013\ t^{-0.0606} \qquad (16)$$

The equation has a correlation factor of -0.916. The similarity in the coefficients for equations (14) and (16) indicates that a relation between the critical current density and the anode surface area does not exist within the range studied, as some other researchers have stated. The slight difference in the current densities obtained with the coupons and the bucket can be explained by what other researchers (22) have found, which is that the magnitude of i_{crit} increases with increasing cathodic pretreatment time. The coupons were not given a cathodic pretreatment; however, the buckets were given a 5 minutes cathodic pretreatment at -500 mV versus SCE. This then explains the difference in the data. The causes for this increase in i_{crit} are not understood at this time (22).

The data for 67 percent H_2SO_4 in the carbon steel bucket is shown in Figure 24. This data is similar to the data for 67 percent H_2SO_4 in the stainless steel bucket. This pattern was also observed with the carbon and stainless steel coupons, as pointed out earlier. Larger varia-

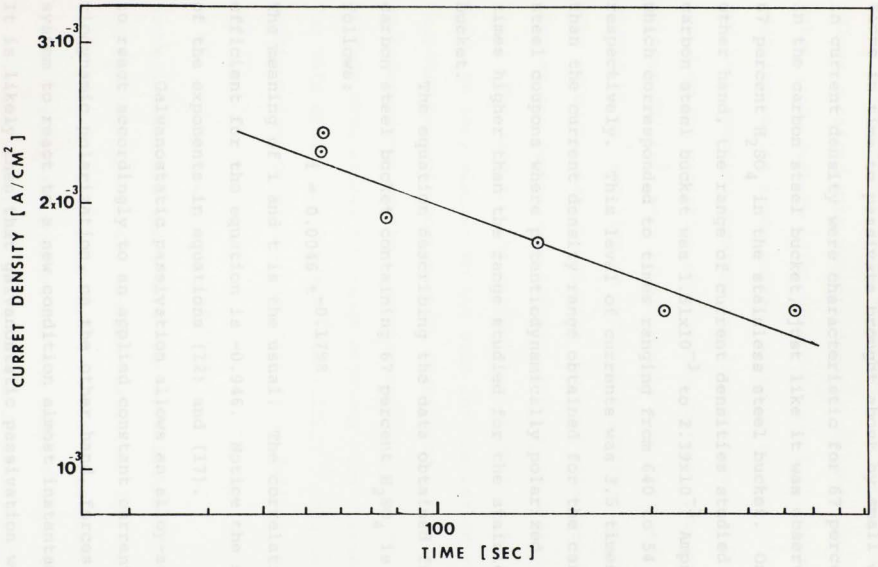

Figure 24 - Log-log plot of i_{crit} versus Time to Passivation for the Galvanostatic Passivation Data for AISI 1018 Carbon Steel Bucket and 67% H_2SO_4.

tions in time to passivate brought about by small changes in current density were characteristic for 67 percent H_2SO_4 in the carbon steel bucket, just like it was observed for 67 percent H_2SO_4 in the stainless steel bucket. On the other hand, the range of current densities studied for the carbon steel bucket was 1.51×10^{-3} to 2.39×10^{-3} Amps/cm^2 which corresponded to times ranging from 640 to 54 seconds, respectively. This level of currents was 3.5 times lower than the current density range obtained for the carbon steel coupons where potentiodynamically polarized, and two times higher than the range studied for the stainless steel bucket.

The equation describing the data obtained from the carbon steel bucket containing 67 percent H_2SO_4 is as follows:

$$i = 0.0046\ t^{-0.1798} \qquad (17)$$

The meaning of i and t is the usual. The correlation coefficient for the equation is -0.946. Notice the similarity of the exponents in equations (12) and (17).

Galvanostatic passivation allows an alloy-acid system to react accordingly to an applied constant current; potentiodynamic polarization, on the other hand, forces the system to react to a new condition almost instantaneously. It is likely then that galvanostatic passivation would yield results closer to equilibrium than potentiodynamic polarization. If this is true, then current densities obtained

under galvanostatic passivation would be lower than the values obtained with potentiodynamic polarization. On the other hand, Sudbury (13) observed that i_{crit} decreased with increasing anode surface areas up to 200 in^2 (1290 cm^2) and then remained constant for larger areas. This work did not show the variation observed by Sudbury for areas smaller than 200 in^2; very close results were obtained with areas of 661.15 cm^2 and 1140.42 cm^2. This affirmation is made more relevant with the results obtained with carbon steel coupons and bucket with 93 percent H_2SO_4 as discussed next.

The data for the carbon steel bucket in 93 percent H_2SO_4 is very similar to the data for the carbon steel coupons when galvanostatically passivated. This indicates an independence of the current density (i_{crit}) on the anode surface area within the range studied. The current range for this system was 2.27×10^{-4} to 1.82×10^{-3} Amps/cm^2. The equation that describes this data is as follows (see Figure 25)

$$i = 0.0106\ t^{-0.6096} \qquad (18)$$

where i and t are the usual. The correlation coefficient for the line is -0.965. Current densities for the carbon steel bucket and coupons were 3 to 3.5 times lower than the current densities obtained for the coupons when potentiodynamically polarized. Here again, it is evident that the anode surface area does not affect the current density; instead, it is the polarization technique used. Finally,

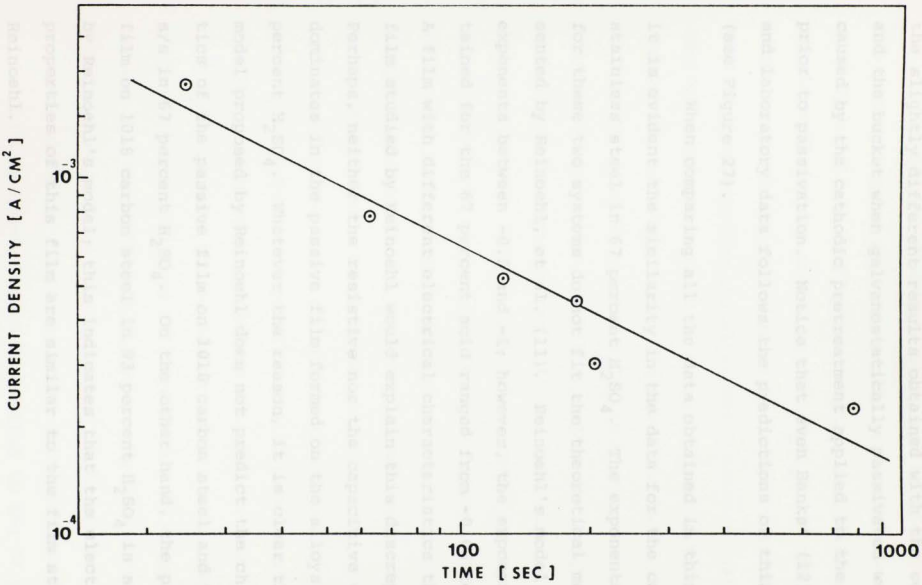

Figure 25 - Log-log Plot of i_{crit} versus Time to Passivation for the Galvanostatic Passivation Data for AISI 1018 Carbon Steel Bucket and 93% H_2SO_4.

the slightly different results obtained with the coupons and the bucket when galvanostatically passivated were caused by the cathodic pretreatment applied to the bucket prior to passivation. Notice that even Banks' (12) field and laboratory data follows the predictions of this study (see Figure 27).

When comparing all the data obtained in this study, it is evident the similarity in the data for the carbon and stainless steel in 67 percent H_2SO_4. The exponents obtained for these two systems do not fit the theoretical model presented by Reinoehl, et al. (11). Reinoehl's model predicts exponents between -0.5 and -1; however, the exponents obtained for the 67 percent acid ranged from -0.06 to -0.18. A film with different electrical characteristics than the film studied by Reinoehl would explain this discrepancy. Perhaps, neither the resistive nor the capacitive character dominates in the passive film formed on the alloys in 67 percent H_2SO_4. Whatever the reason, it is clear that the model proposed by Reinoehl does not predict the characteristics of the passive film on 1018 carbon steel and Type 316 s/s in 67 percent H_2SO_4. On the other hand, the passive film on 1018 carbon steel in 93 percent H_2SO_4 is simulated by Reinoehl's model; this indicates that the electrical properties of this film are similar to the film studied by Reinoehl.

The results form this study can be used to analyze the possibility of applying anodic protection to the systems Type 316 s/s in 67 percent H_2SO_4, and 1018 carbon steel in 67 percent and 93 percent H_2SO_4. On one hand, there is no use in saving money by using low current densities to passivate the stainless steel because almost instantaneous passivation could be obtained by supplying a few amperes more for big tanks. On the other hand, if one decides to store 93 percent H_2SO_4 in a carbon steel tank, the time to passivate it will depend on how frequently on tank has to be repassivated. If the tank remains passive for long periods (2-3 months), then longer passivating times may be selected; however, if the tank is very unstable (activates back quickly), then short passivating times should be selected. It is worthy of note that carbon steel in 93 percent has a tendency to self-passivate, this in part explains the lower current densities needed to passivate this system as compared to the 67 percent acid case. Finally, carbon steel tanks are not used to store 67 percent H_2SO_4 because the corrosion rates are too high. The purpose of the data from this system was to compare results between the two different alloys in the same environment. The comparison would have been done in 93 percent H_2SO_4; however, since the stainless steel self-passivates in this acid, the comparison had to be limited to the 67 percent concentration only.

A summary of the data obtained for carbon steel and Type 316 s/s in 67 percent H_2SO_4 is presented in Table 3 and Figure 26. As said before, the data for both systems yielded very similar relations as it is evident from the almost parallel curves shown in Figure 26. The difference in the current level is mainly due to the increased stability inherited by the stainless steel from its alloy constituents. On the other hand, the data for carbon steel in 93 percent H_2SO_4 is shown in Figure 27 and is summarized on Table 3. Notice that Banks' (12) data has also been included to point out the closeness of this data to the predictions of this study. From this summary, it can be concluded that i_{crit} depends on the time to passivate and vice versa, but not on the anode surface area, as stated by earlier researchers.

Table 3

The equations describing the data obtained in this study are of the form:

$$i = at^b$$

Alloy/Acid Conc.	Polarization Technique	Anode	a	b	r*
316 s/s 67%	Potentiodynamic	Coupons	0.00132	-0.1781	-0.973
316 s/s 67%	Galvanostatic	Coupons	0.00116	-0.0763	-0.987
316 s/s 67%	Galvanostatic	Bucket	0.00130	-0.0606	-0.916
1018 cs 67%	Potentiodynamic	Coupons	0.0151	-0.1680	-0.843
1018 cs 67%	Galvanostatic	Bucket	0.0046	-0.1798	-0.946
1018 cs 93%	Potentiodynamic	Coupons	0.0430	-0.6177	-0.994
1018 cs 93%	Galvanostatic	Coupons	0.01437	-0.6495	-0.991
1018 cs 93%	Galvanostatic	Bucket	0.0106	-0.6096	-0.965

*correlation coefficient as calculated with the Least Squares Method.

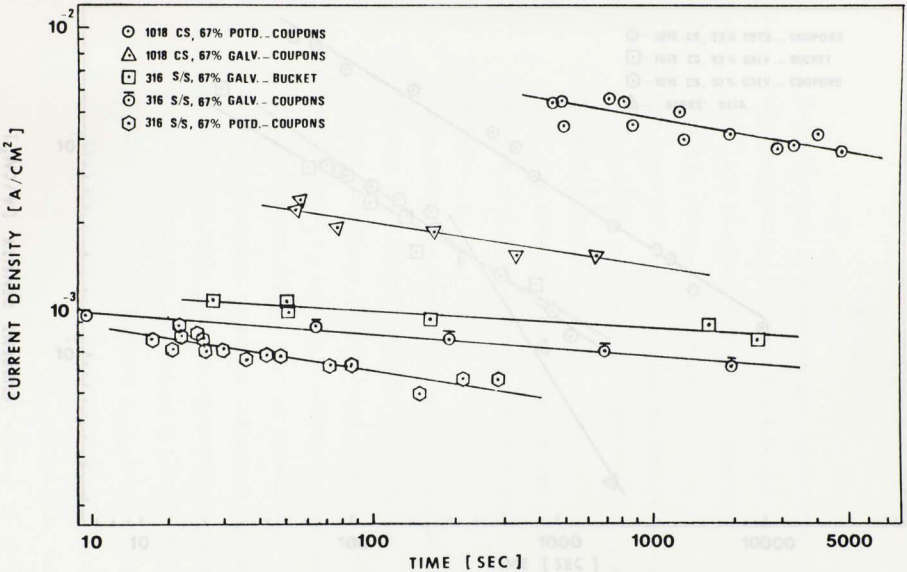

Figure 26 - Summary of Data for Type 316 s/s and AISI 1018 Carbon Steel and 67% H_2SO_4.

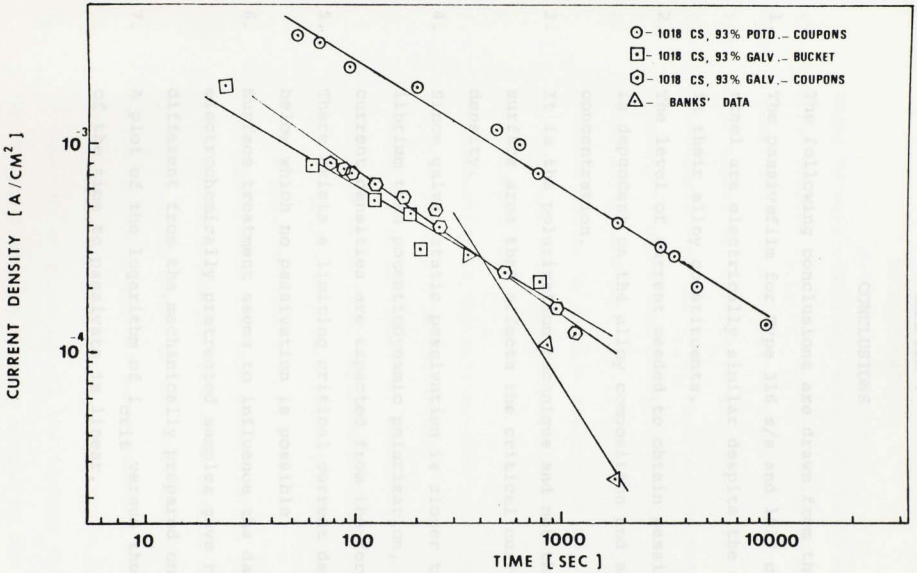

Figure 27 - Summary of Data for AISI 1018 Carbon Steel and 93% H_2SO_4, and Banks' Field Data.

CHAPTER V

CONCLUSIONS

The following conclusions are drawn from this study:

1. The passivefilm for Type 316 s/s and 1018 carbon steel are electrically similar despite the difference in their alloy constituents.
2. The level of current needed to obtain passivation is dependent on the alloy composition and acid concentration.
3. It is the polarization technique and not the anode surface area that affects the critical current density.
4. Since galvanostatic passivation is closer to equilibrium than potentiodynamic polarization, lower current densities are expected from the former.
5. There exists a limiting critical current density below which no passivation is possible.
6. Surface treatment seems to influence the data since electrochemically pretreated samples gave results different from the mechanically prepared ones.
7. A plot of the logarithm of i_{crit} versus the logarithm of the time to passivate is linear.

CHAPTER VI

RECOMMENDATIONS

There is much additional work that can be done on the relation between i_{crit} for anodic protection and the time to passivate. Some suggested areas for further investigation of topics not covered in this study are:

1. Investigation of the i_{crit}-time-to-passivate relationship in other acid concentrations.
2. Other alloys and pure metals (Ni, Cr, etc.) should be investigated to enforce the conclusion that the current-time relation exponent is independent of alloy composition.
3. The dependence of the current-time relation on temperature should be researched.
4. A technique to determine the electrical properties of passive films (a.c. impedance) should be used in order to determine a more realistic electrical model for the passive films studied.
5. Experiments using the same potentiostat, or same polarization technique, should be carried out for different anode areas to make sure that the polarization technique and not other variable affects the critical current density.
6. An equation correlating all the factors that affect the critical current density should be the aim for future work to be done on this topic.

REFERENCES

1. Mars G. Fontana and Norbert D. Greene, Corrosion Engineering, McGraw-Hill, Inc., New York, 1978.

2. Olen L. Riggs, Jr. and Carl E. Locke, Anodic Protection, Plenum Press, New York, 1981.

3. Z. A. Foroulis, Corrosion Science, 5, 383-391 (1965).

4. J. E. Reinoehl and F. H. Beck, Corrosion, 25, 233-240 (1969).

5. Herbert H. Uhligh, Corrosion and Corrosion Control, 2nd ed., John Wiley & Sons Inc., New York, 1971.

6. John O'M. Bockris and Amulya K. N. Reddy, Modern Electrochemistry, Volume 2, Plenum Press, New York, 1970.

7. ASTM Committee G-1 Subcommittee XI Task Group 2, W. D. France, Jr., Chairman, "Recommended Practice for a Standard Method for Making Potentiostatic and Potentiodynamic Polarization Measurements" (1968).

8. Z. A. Foroulis, Ind. Eng. Chem. Process Des. Dev. 4, 20-23 (1965).

9. Z. A. Foroulis, Ind. Eng. Chem. Process Des. Dev. 4, 23-25 (1965).

10. W. A. Mueller, Corrosion, 18, 73t-78t (1962).

11. J. E. Reinoehl, F. H. Beck, and M. G. Fontana, Corrosion, 26, 141-150 (1970).

12. W. P. Banks and J. D. Sudburry, Corrosion, 19, 300t-307t (1963).

13. J. D. Sudbury, O. L. Riggs, and D. A. Shock, Corrosion, 16, 47t-54t (1960).

14. C. J. Chatfield and L. L. Shreir, Corrosion Science, 12, 563-570 (1972).

15. A. B. Ijzermans, Corrosion Science, 10, 113-117 (1970).

16. N. D. Greene and R. B. Leonard, Electrochim. Acta, 9, 45-54 (1964).

17. H. J. Engell and B. Ilsehner, Z. Elektrochemie, 59, 716-722 (1955).

18. M. Afzal, "The Study of the Passive film on Nickel-200 and Inconel X-750", Master Dissertation, the University of Oklahoma (1975).

19. N. D. Greene, W. D. France, Jr., and B. E. Wilde, Corrosion, 21, 275-276 (1965).

20. N. D. Greene, Experimental Electrode Kinetics, Ph.D. Dissertation, Rensselaer Polytechnic Institute, Troy, New York, 1965.

21. R. C. Williamson and J. G. Hines, Corrosion Science, 4, 221-235 (1964).

22. C. D. Kim and B. E. Wilde, Corrosion Science, 10, 735-744 (1970).

23. Carl E. Locke, personal communication.